UC San Diego
UC San Diego Previously Published Works

Title

Functional magnetic resonance imaging for in vivo quantification of pulmonary hypertension in the Sugen 5416/hypoxia mouse

Permalink

https://escholarship.org/uc/item/0mn5j21b

Journal

Experimental Physiology, 102(3)

ISSN

0958-0670

Authors

Breen, Ellen C
Scadeng, Miriam
Lai, N Chin
et al.

Publication Date

2017-03-01

DOI

10.1113/ep086067

Peer reviewed

Research Paper

Functional magnetic resonance imaging for *in vivo* quantification of pulmonary hypertension in the Sugen 5416/hypoxia mouse

Ellen C. Breen[1] (iD), Miriam Scadeng[2], N. Chin Lai[3], Fiona Murray[4] and The Late Timothy D. Bigby[1,3]

[1]*Medicine, University of California, San Diego, La Jolla, CA, USA*
[2]*Radiology, University of California, San Diego, La Jolla, CA, USA*
[3]*Pulmonary & Critical Care, Veterans Administration San Diego, La Jolla, CA, USA*
[4]*Medicine, University of Aberdeen, Aberdeen, UK*

Edited by: Karin Przyklenk

Experimental Physiology

New Findings
- **What is the central question of this study?**
  Non-invasive, quantitative methods to assess right cardiac function in mice with pulmonary hypertension have not been demonstrated.
- **What is the main finding and its importance?**
  This study shows the potential of magnetic resonance imaging to estimate right ventricular ejection fraction and measure spatial, dynamic changes in cardiac structure in the Sugen 5416/hypoxia mouse model of pulmonary hypertension.

Pulmonary arterial hypertension (PAH) is characterized by elevated pulmonary artery pressures and right heart failure. Mouse models of PAH are instrumental in understanding the disease pathophysiology. However, few methods are available to evaluate right cardiac function in small animals. In this study, magnetic resonance imaging was used to measure *in vivo* cardiac dimensions in the Sugen 5416/hypoxia mouse model. Pulmonary hypertension (PH) was induced in C57BL/6 mice by 3 weeks of exposure to 10% oxygen and vascular endothelial growth factor receptor inhibition (20 mg kg^{-1} SU5416). Control mice were housed in room air and received vehicle (DMSO). Right ventricular pressures were recorded with a pressure-conductance transducer. Short-axis contiguous 1-mm-thick slices were acquired through the heart and great vessels using a fast low-angle shot (FLASH)-cine sequence. Thirteen images were collected throughout each cardiac cycle. Right ventricular systolic pressure was elevated in PH mice (23.6 ± 6 *versus* 41.0 ± 11 mmHg, control *versus* PH, respectively; $P < 0.001$, $n = 5$–11). Right ventricular wall thickness was greater in PH than in control mice at end diastole (0.30 ± 0.05 *versus* 0.48 ± 0.06 mm, control *versus* PH, respectively; $P < 0.01$, $n = 6$), but measurements were not different at end systole (control *versus* PH, 0.59 ± 0.11 *versus* 0.70 ± 0.11 mm, respectively). Right ventricular ejection fraction was decreased in PH mice (72 ± 3 *versus* 58 ± 5%, control *versus* PH, respectively; $P < 0.04$, $n = 6$). These data demonstrate that magnetic resonance imaging is

E. C. Breen and M. Scadeng contributed equally to this study.

Corresponding author E. C. Breen: Department of Medicine, University of California, San Diego, 9500 Gilman Drive, La Jolla, CA 92093-0623, USA. Email: ebreen@ucsd.edu

Introduction

Pulmonary arterial hypertension (PAH) is a multifactorial disorder that is characterized by remodelling of the small muscular arteries, increased pulmonary vascular resistance and right heart failure (Rabinovitch, 2012; Simonneau *et al.* 2013). Right ventricular (RV) pressures are elevated in PAH, and the heart structure (wall thickness, capillarity and collagen content; Rabinovitch *et al.* 1986; Janssen *et al.* 2015) and metabolic profile are altered (Mouchaers *et al.* 2009; Paulin & Michelakis, 2014). Measurements of *in vivo* cardiac function and structural changes in small (25–30 g) animal models require precise, non-invasive imaging methods. Current methods to evaluate these changes in cardiac structure and function in mouse models of pulmonary hypertension (PH) include echocardiography, pressure recordings within the right ventricle, assessment of ventricular weights and standard histology. However, these methods are technically difficult and limited in scope (Gomez-Arroyo *et al.* 2012). As functional magnetic resonance imaging (MRI) becomes more available in research settings, the potential exists non-invasively to capture two- or three-dimensional images of the heart that are gated to the cardiac cycle. Recently, MRI-based dynamic methods have been used to assess right heart function in transgenic mice (Novoyatleva *et al.* 2013; Szema *et al.* 2013; Hillestad *et al.* 2015) and in mice that have been subjected to a physiological challenge, such as exposure to chronic hypoxia (Poels *et al.* 2014; Hillestad *et al.* 2015) or pressure overload (Novoyatleva *et al.* 2013; Janssen *et al.* 2015).

The current preclinical mouse model of PAH, which is thought to resemble human PAH closely, combines administration of the vascular endothelial growth factor receptor inhibitor SU5416 with exposure to chronic hypoxia (Tuder *et al.* 1994; Taraseviciene-Stewart *et al.* 2001; Vitali *et al.* 2014). This model of PH allows for the use of transgenic mice to elucidate the underlying mechanisms leading to pulmonary and cardiac remodelling. To assess cardiac functional changes in mice with Sugen 5416/hypoxia-induced PH by MRI, we used a high-field-strength 7 T magnet and gated T1-weighted imaging to collect a series of contiguous cross-sectional cinematic images of the heart throughout the cardiac cycle. These images closely reflect the real-time (resolution of 20–30 ms) *in vivo* dimensions of a functioning heart. The volumes of the right ventricle at end systole and end diastole were recorded from the images, and the difference in volume was used as an estimate of the ejection fraction. The thickness of the right ventricular wall was also measured at these time points as an indication of right ventricular wall remodelling. Our data show that MRI provides a method to monitor, non-invasively and longitudinally, the changes in the right heart function of mice with Sugen 5416/hypoxia-induced PH. Such a methodology could be used in transgenic mice to help elucidate the mechanisms that contribute to PAH and right heart failure.

Methods

Animals

All studies were performed according to National Institutes of Health *Guidelines for the Care and Use of Laboratory Animals* (available at https://grants.nih.gov/grants/olaw/guide-for-the-care-and-use-of-laboratory-animals.pdf) and approved by the institutional animal care and use committee of the Veterans Administration San Diego Healthcare System. Male C57BL/6 mice (3 months of age) from Jackson Laboratories (Bar Harbor, ME, USA) were used for this study. Mice were fed Teklad 7001 standard diet from Harlan Laboratories (Madison, WI, USA) *ad libitum*.

Sugen 5416/hypoxia mouse

Pulmonary hypertension was induced in C57BL/6 mice by exposure to normobaric 10% O_2 plus weekly s.c. injections of SU5416 (20 mg kg^{-1} in DMSO) for 3 weeks. Control mice were housed in room air and were administered vehicle (DMSO) each week for 3 weeks.

Functional MRI

Mice were anaesthetized with 1.25% isoflurane through a nose cone and allowed to breathe 21% O_2 spontaneously throughout the imaging period. Body temperature was monitored and maintained at 37°C. Each mouse was positioned in the magnet coil, and ECG leads were attached. The imaging sequence was triggered by R wave detection of each cardiac cycle. A pulse oximeter (MouseOx Plus; Starr Life Science Corp., Oakmont, PA, USA) was used to monitor O_2 saturation (control, 95.5 $\pm$ 1.8%; PAH, 94.9 $\pm$ 0.5%; P = n.s., n = 6), heart rate (control, 512 $\pm$ 15 beats min^{-1}; PAH,

482 ± 18 beats min^{-1}; P = n.s., n = 6) and breathing rate (control, 110 ± 5 breaths min^{-1}; PAH, 95 ± 7 breaths min^{-1}; P = n.s., n = 6). Magnetic resonance images were collected using a Bruker 7 T small animal scanner with a 2.5 mm volume coil and a fast low-angle shot (FLASH-cine; echo time, 2.11 ms; and relaxation time, 8 ms) pulse sequence. Gated images were collected through the short axis at 1 mm intervals to include the great vessels and extended through to the apex of the heart. Image resolution was 150 μm × 133 μm. Thirteen cinematic images were collected throughout each cardiac cycle. The average interval between images was ∼9 ms. For quantification, the internal cardiac margins were delineated by blood (high intensity) in the heart chambers and the external margins delineated by the air in the lung. For delineation of the ventricular volume, the upper level cut-off was the tricuspid valve. The slice with the tricuspid valve usually contained predominantly atrium and was, therefore, not used in the ventricular volume assessment. Segmentation was performed using Amira software (Thermo Fisher Scientific, Waltham, MA, USA), and volumes were calculated from the number of voxels selected multiplied by the voxel volume.

In vivo RV pressure measurements

The right ventricular chamber was accessed by way of Sastry *et al.* (2006) with a small pressure-conductance transducer. Briefly, general anaesthesia was induced in mice with 5% isoflurane, and they were placed on a water-filled warming pad and ventilated mechanically with 1.5% isoflurane admixed with 1 l min^{-1} oxygen. An incision was made in the ventral mid-line of the neck, and the right jugular vein was exposed by blunt dissection. A distal tie (6–0 silk suture) on the vein was made to serve as a retractor while a loose silk knot was placed at the proximal end that was used to occlude the vein temporarily. A small incision was made between the two sutures, and a 1.4 French pressure-conductance transducer (Millar SPR-839) was inserted and advanced into the vessel and to the RV cavity. The catheter was secured by the proximal suture once RV pressure waveform was identified. Right ventricular pressures were recorded, converted digitally via an analog-to-digital converter (IOX 1.8; emka Technologies, Falls Church, VA, USA), and stored on a computer for analyses. Upon completion of data collection, the mouse was killed with an overdose of isoflurane (5%).

Statistical analyses

Student's unpaired, two-tailed t test was used to compare the control (vehicle/room air) and PH (Sugen 5416/hypoxia) groups. A two-way ANOVA was used to compare the wall thickness at both end diastole and end systole between the experimental groups. Sidak's *post hoc* test was used for multiple comparisons. Data are represented as the means ± SD. A value of $P \leq 0.05$ was considered a significant difference.

Results

Body weights

The PH group weighed significantly less (9.8%) than the control group (24.5 ± 1.8 *versus* 22.1 ± 1.1 g, control *versus* PH, respectively; P < 0.03, n = 6).

Estimate of cardiac function from dynamic MRI

The wall motion, observed cinematically (displayed in movie format in Supplemenary material, Movies S1 and S2), revealed irregular motion during the cardiac cycle in the PH mice. Changes in the static structure of the heart are presented in Fig. 1. The PH hearts are larger and more distended at both end systole and end diastole than the control hearts. Segmentation of the volume in each imaged slice of the right ventricle was added together to determine the total ventricular volume. Measurements were collected from images captured at end systole and end diastole. The difference in these two volumes is an estimate of the volume of blood ejected from the heart. Ejection fractions were 20% lower in the PH group than the control group (71.9 ± 6 *versus* 57.6 ± 13%, control *versus* PH, respectively; P < 0.04, n = 6; Fig. 2A). As an indication that the heart was adapting or remodelling in response to the increased pressure, the thickness of the right lateral wall of the right ventricle was measured (Fig. 2B). Measurements were taken from images of the upper region of the ventricle (∼6 mm from the base of the heart). A 60% increase in the width of the right lateral wall was observed in the PH group when measurements were taken at end diastole (0.30 ± 0.05 *versus* 0.48 ± 0.06 mm, control *versus* PH, respectively; P < 0.01, n = 6), but no differences in wall thickness were detected at end systole (0.59 ± 0.11 *versus* 0.70 ± 0.11 mm, control *versus* PH, respectively; n = 6).

Estimates of cardiac function by *in vivo* pressure recordings

Right ventricular systolic pressures, measured by placement of a pressure-conductance catheter, revealed an increase in the PH group (23.6 ± 6 *versus* 41.0 ± 11 mmHg, control *versus* PH; P < 0.001, n = 5–11; Fig. 3A). Heart rates were not different between the two experimental groups (605 ± 121 *versus* 573 ± 65 beats min^{-1}, control *versus* PH, respectively; P = 0.61, n = 7 and 5, respectively; Fig. 3B). A trend for a change in RV +dP/dt, the instantaneous rate of contraction (2367 ± 829 *versus*

3242 ± 903 mmHg s^{-1}, control *versus* PH, respectively; $P < 0.08$, $n = 11$ and 5, respectively, Fig. 3*C*) and difference in RV $-\mathrm{d}P/\mathrm{d}t$, the instantaneous rate of relaxation (-2085 ± 657 *versus* -2859 ± 718 mmHg s^{-1}, control *versus* PH, respectively; $P = 0.052$, $n = 11$ and 5, respectively; Fig. 3*D*) were detected.

Discussion

Our data demonstrate the usefulness of functional magnetic resonance imaging for evaluating the structure and function of the right heart in the Sugen 5416/hypoxia mouse model of PH. Measurement of right heart anatomy is particularly difficult with echocardiography; however, cinematic MRI provides a powerful tool to characterize both the structure and the function of the right heart in mouse models of PH. We found that in Sugen 5416/hypoxia mice, the cardiac ejection fraction was on average 20% lower than in control mice.

This index of cardiac function could then be reported with dynamic measurements of right ventricular wall thickness measured throughout the cardiac cycle. In Sugen 5416/hypoxia mice, the right ventricular thickness measured during end diastole was increased by 60% above control values. One limitation of this analysis is that corresponding wall dimensions were not measured *ex vivo* in hearts fixed at pressures that reflect end diastole. However, the collected data demonstrate that this method is able to correlate *in vivo* indices of cardiac remodelling with cardiac output using a non-invasive measurement, which is ideal for longitudinal study designs.

Magnetic resonance imaging cardiac output measurements to evaluate right heart failure

Data from our control or normal C57BL/6J mice are in good agreement with similar measurements of cardiac function reported in other studies. Buonincontri
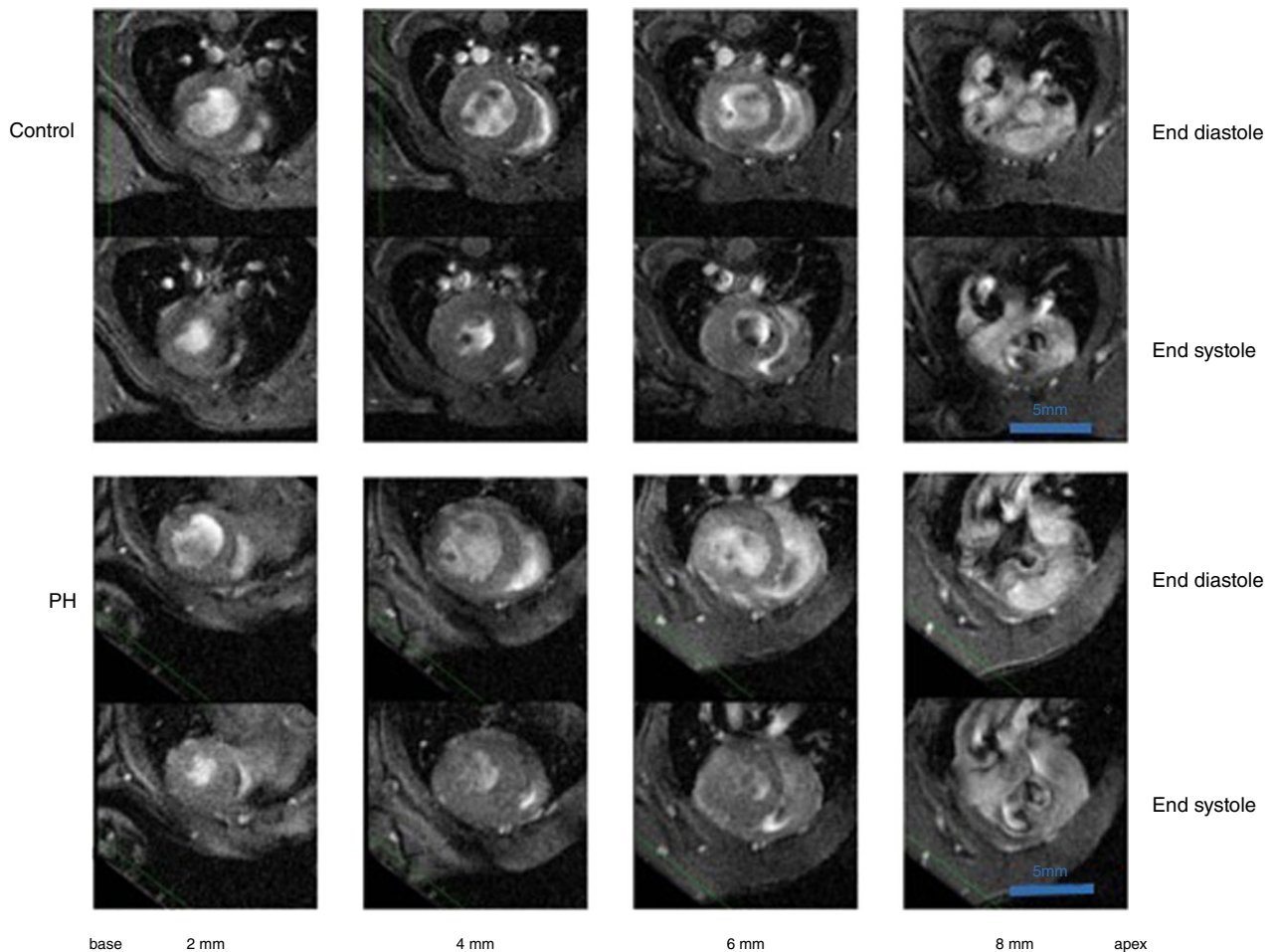

Figure 1. Representative axial images of the heart from the base to the apex are presented at end systole and end diastole in mice maintained in control conditions or with induced pulmonary hypertension (PH)
The control mice were maintained in room air. The PH mice were exposed to 10% O$_2$ and received weekly s.c. injections of SU5416 (20 mg kg^{-1}). The distance from the base of the heart is labelled (in millimetres).

et al. (2014) reported a 71% ejection fraction, which is similar to the 67.7% average ejection fraction that was observed in the control group of C57BL/6J mice in our study. The study also reported a progressive decrease in ejection fraction in RB/2 mice, a model of Huntington's disease, that correlated with large increases

in right ventricular end-systolic volume upon dobutamine challenge (Buonincontri *et al.* 2014). In another model of right heart failure, induced via pulmonary artery banding for 3 weeks, the right ventricular pressures increased from 28.1 to 63 mmHg (Novoyatleva *et al.* 2013). Such a large increase in pressure corresponded to a 35% decrease in
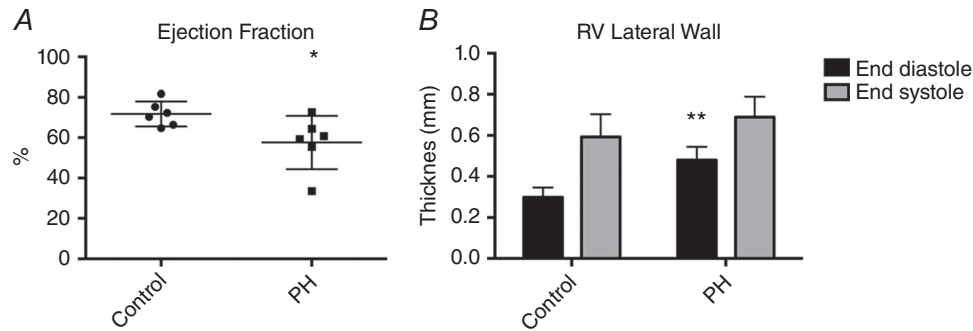

Figure 2. Functional magnetic resonance imaging measurements of ejection fractions and right ventricular lateral wall thickness
A, the ejection fraction was estimated by segmentation of right ventricular volumes from the contiguous images collected by magnetic resonance imaging. $n = 6$ mice per group. Data are the means $\pm$ SD; *$P < 0.05$. *B*, measurements of wall thickness were made at the uppermost region of the ventricle from images collected at both end systole and end diastole in control mice and hypoxia/SU546 mice. **$P < 0.01$, difference between control and PH mice at end diastole, means $\pm$ SD, $n = 6$ mice per group.
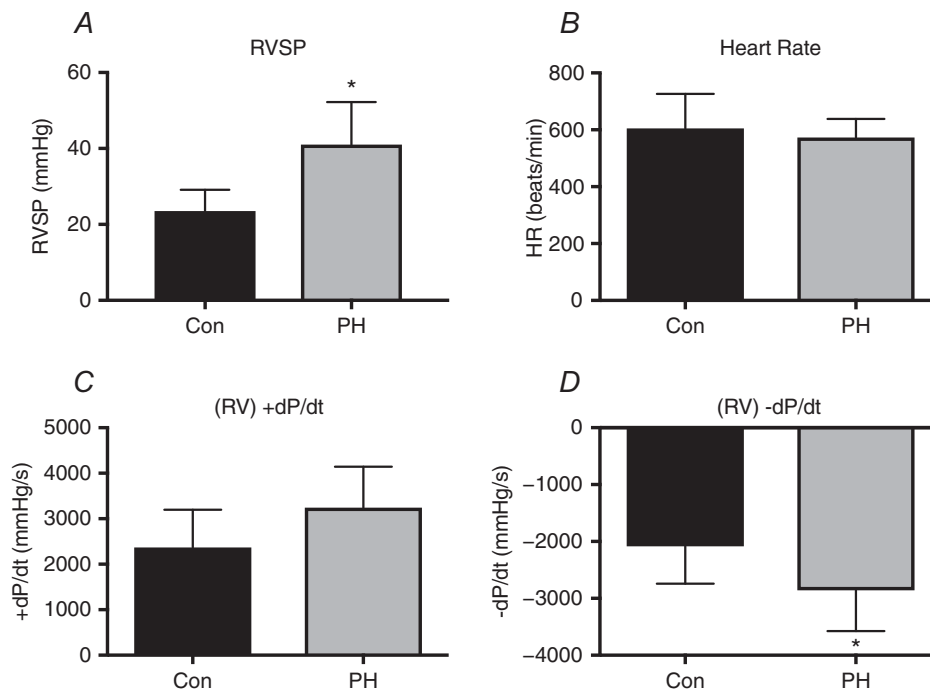

Figure 3. Invasive pressure recordings
Right ventricular (RV) pressures were measured with a Millar 1.4 French solid-state pressure catheter and are expressed as follows: RV end-systolic pressure (RVSP; *A*); mean heart rate (*B*, instantaneous rate of contraction); (RV) +d*P*/d*t* (*C*); and (RV) −d*P*/d*t* (*D*, instantaneous rate of relaxation). Data are represented as the means $\pm$ SD. Control (Con), $n = 11$; and PH, $n = 5$. *$P \leq 0.05$.

cardiac output measured by MRI, which was higher than the 20% decrease in MRI-estimated cardiac output in the present PH model (Novoyatleva *et al.* 2013). Magnetic resonance imaging has also been used for analysis of cardiac function in vasoactive intestinal peptide knockout ($Vip^{-/-}$) mice (Szema *et al.* 2013). Right ventricular diastolic volume was used to phenotype the $Vip^{-/-}$ mice, which was accompanied by an increase in right and left ventricular chamber size compared with control mice. Together with the present study, these data further illustrate the sensitivity and reproducibility of using MRI for measuring both cardiac structure and function of the right heart.

In the present study, both cardiac output and anatomical measurements were collected from the imaging data in the Sugen 5416/hypoxia mouse. Collecting a series of images that both span the heart beat of a mouse and provide three-dimensional information results in an enormous amount of information that can be used to test the mechanistic function of these changes in transgenic models. This type of cardiac functional phenotyping may even pave the way for further analysis of dynamic mechanics of the heart in patients suffering from PAH.

References

Buonincontri G, Wood NI, Puttick SG, Ward AO, Carpenter TA, Sawiak SJ & Morton AJ (2014). Right ventricular dysfunction in the R6/2 transgenic mouse model of Huntington's disease is unmasked by dobutamine. *J Huntingtons Dis* **3**, 25–32.

Gomez-Arroyo J, Saleem SJ, Mizuno S, Syed AA, Bogaard HJ, Abbate A, Taraseviciene-Stewart L, Sung Y, Kraskauskas D, Farkas D, Conrad DH, Nicolls MR & Voelkel NF (2012). A brief overview of mouse models of pulmonary arterial hypertension: problems and prospects. *Am J Physiol Lung Cell Mol Physiol* **302**, L977–L991.

Hillestad V, Espe EK, Cero F, Larsen KO, Sjaastad I, Nygård S, Skjønsberg OH & Christensen G (2015). IL-18 neutralization during alveolar hypoxia improves left ventricular diastolic function in mice. *Acta Physiol (Oxf)* **213**, 492–504.

Janssen W, Schymura Y, Novoyatleva T, Kojonazarov B, Boehm M, Wietelmann A, Luitel H, Murmann K, Krompiec DR, Tretyn A, Pullamsetti SS, Weissmann N, Seeger W, Ghofrani HA & Schermuly RT (2015). 5-HT2B receptor antagonists inhibit fibrosis and protect from RV heart failure. *Biomed Res Int* **2015**, 438403.

Mouchaers KT, Schalij I, Versteilen AM, Hadi AM, van Nieuw Amerongen GP, van Hinsbergh VW, Postmus PE, van der Laarse WJ & Vonk-Noordegraaf A (2009). Endothelin receptor blockade combined with phosphodiesterase-5 inhibition increases right ventricular mitochondrial capacity in pulmonary arterial hypertension. *Am J Physiol Heart Circ Physiol* **297**, H200–H207.

Novoyatleva T, Janssen W, Wietelmann A, Schermuly RT & Engel FB (2013). TWEAK/Fn14 axis is a positive regulator of cardiac hypertrophy. *Cytokine* **64**, 43–45.

Paulin R & Michelakis ED (2014). The metabolic theory of pulmonary arterial hypertension. *Circ Res* **115**, 148–164.

Poels EM, Bitsch N, Slenter JM, Kooi ME, de Theije CC, de Windt LJ, van Empel VP & da Costa Martins PA (2014). Supplementing exposure to hypoxia with a copper depleted diet does not exacerbate right ventricular remodeling in mice. *PLoS One* **9**, e92983.

Rabinovitch M (2012). Molecular pathogenesis of pulmonary arterial hypertension. *J Clin Invest* **122**, 4306–4313.

Rabinovitch M, Bothwell T, Hayakawa BN, Williams WG, Trusler GA, Rowe RD, Olley PM & Cutz E (1986). Pulmonary artery endothelial abnormalities in patients with congenital heart defects and pulmonary hypertension. A correlation of light with scanning electron microscopy and transmission electron microscopy. *Lab Invest* **55**, 632–653.

Sastry A, Arnold E, Gurji H, Iwasa A, Bui H, Hassankhani A, Patel HH, Feramisco JR, Roth DM, Lai NC, Hammond HK & Narayan SM (2006). Cardiac-directed expression of adenylyl cyclase VI facilitates atrioventricular nodal conduction. *J Am Coll Cardiol* **48**, 559–565.

Simonneau G, Gatzoulis MA, Adatia I, Celermajer D, Denton C, Ghofrani A, Gomez Sanchez MA, Krishna Kumar R, Landzberg M, Machado RF, Olschewski H, Robbins IM & Souza R (2013). Updated clinical classification of pulmonary hypertension. *J Am Coll Cardiol* **62**, D34–D41.

Szema AM, Hamidi SA, Smith SD & Benveniste H (2013). VIP gene deletion in mice causes cardiomyopathy associated with upregulation of heart failure genes. *PLoS One* **8**, e61449.

Taraseviciene-Stewart L, Kasahara Y, Alger L, Hirth P, Mc Mahon G, Waltenberger J, Voelkel NF & Tuder RM (2001). Inhibition of the VEGF receptor 2 combined with chronic hypoxia causes cell death-dependent pulmonary endothelial cell proliferation and severe pulmonary hypertension. *FASEB J* **15**, 427–438.

Tuder RM, Groves B, Badesch DB & Voelkel NF (1994). Exuberant endothelial cell growth and elements of inflammation are present in plexiform lesions of pulmonary hypertension. *Am J Pathol* **144**, 275–285.

Vitali SH, Hansmann G, Rose C, Fernandez-Gonzalez A, Scheid A, Mitsialis SA & Kourembanas S (2014). The Sugen 5416/hypoxia mouse model of pulmonary hypertension revisited: long-term follow-up. *Pulm Circ* **4**, 619–629.

Additional information

Competing interests

Author contributions

E.C.B., M.S., N.C.L. and F.M. All authors approved the final version of the manuscript and agree to be accountable for all aspects of the work in ensuring that questions related to the accuracy or integrity of any part of the work are appropriately investigated and resolved. All persons designated as authors qualify for authorship, and all those who qualify for authorship are listed.

Supporting information

Supporting Movie S1: Dynamic imaging of the right ventricle during the cardiac cycle in a control mouse.
Supporting Movie S2: Dynamic imaging of the right ventricle during the cardiac cycle in a PH mouse.